Catalysis Today 143 (2009) 261–268

Contents lists available at ScienceDirect

Catalysis Today

journal homepage: www.elsevier.com/locate/cattod

Arsenic (V) removal with nanoparticulate zerovalent iron: Effect of UV light and humic acids

María E. Morgada [a,b], Ivana K. Levy [a,b], Vanesa Salomone [a], Silvia S. Farías [a], Gerardo López [c,d], Marta I. Litter [a,b,e,*]

[a] Gerencia Química, Centro Atómico Constituyentes, Comisión Nacional de Energía Atómica, Buenos Aires, Argentina
[b] Consejo Nacional de Investigaciones Científicas y Técnicas, Argentina
[c] Nanotek S.A., Santa Fe, Argentina
[d] Facultad Regional Santa Fe, Universidad Tecnológica Nacional, Santa Fe, Argentina
[e] Escuela de Posgrado, Universidad Nacional de San Martín, Buenos Aires, Argentina

ARTICLE INFO

Article history:
Available online 26 November 2008

Keywords:
Nanozerovalent iron
Arsenic
UV light
Humic acids

ABSTRACT

Results on As(V) removal in the presence of oxygen using the zerovalent iron technology with commercial iron nanoparticles (NanoFe®) are presented, showing the effect of (NanoFe®) mass, UV light and addition of humic acids. The nanosized iron particles (NZVI) were characterized in their particle size, surface area and constituent phases. As(V) removal was rapid and increased with NZVI mass (0.005–0.1 g L^{-1}) attaining more than 90% after 150 min of time contact with the optimal NanoFe® concentration. The removal followed a biexponential kinetic decay, with rate constants increasing with NZVI mass. (NanoFe®) presented an outstanding ability to remove As due to not only a high surface area and low particle size but also to a high intrinsic activity. Humic acids (HA) decreased around 50% the removal efficiency in the dark, indicating competition with As(V) for active surface sites. In contrast, UV light doubled removal rates, the process being even more enhanced in the presence of HA, with an almost total arsenic removal within 4 h. In all cases, adsorption on iron corrosion phases was found the main mechanism of As(V) removal, promoted by formation of Reactive Oxygen Species and enhanced under UV irradiation by the formation of multiple active species. Preliminary results with As-polluted groundwater of the Chacopampean Plain of Argentina (Tucumán Province) are also reported. Addition of NanoFe® under UV irradiation for 3 h resulted in As contents well in agreement with the regulations (<10 μg L^{-1}).

1. Introduction

Arsenic is a metalloid extremely toxic for animals, human beings and many vegetal species. It is naturally present in groundwaters in the form of different chemical species, coming from leaching of minerals or soils; some anthropic activities, especially mining, contribute artificially to arsenic pollution in groundwater. The presence of As in water for human consumption caused a high incidence of HACRE (Chronic Endemic Regional Hydroarsenicism, *Hidroarsenicismo Crónico Regional Endémico* in Spanish), a hydric disease that produces skin alterations and cancer [1] and affects huge populations, especially in the Asiatic Southeast and Latin America. An extended region of Argentina is affected by the problem, and the country occupies the third place in the world in population at risk for drinking water polluted with arsenic [1,2]. In order to protect population, the World Health Organization (WHO) [3] and most national regulatory agencies, including the Argentine Food Code [4], recommend 10 μg L^{-1} as the maximum allowable arsenic concentration in drinking water.

Predominant forms of As in natural ground- and surface waters (neutral pH) are arsenate (As(V), as oxianions $H_2AsO_4^-$ and $HAsO_4^{2-}$) and arsenite (As(III), as the neutral $H_3AsO_3^0$ species). The mobility of arsenical forms in waters is very dependent on pH, Eh conditions and presence of different chemical species [5]. Consequently, removal methods must take into account these physicochemical properties.

Various methods have been used to remove arsenic from drinking water, including oxidation/coagulation/adsorption on flocs of iron or aluminum hydroxides, anion exchange, precipitation, ion flotation, adsorption on activated alumina, lime softening,

* Corresponding author at: Gerencia Química, Centro Atómico Constituyentes, Comisión Nacional de Energía Atómica, Av. Gral. Paz 1499, 1650 Buenos Aires, Argentina. Tel.: +54 11 6772 7016; fax: +54 11 6772 7886.
E-mail address: litter@cnea.gov.ar (M.I. Litter).

0920-5861/$ – see front matter © 2008 Elsevier B.V. All rights reserved.
doi:10.1016/j.cattod.2008.09.038

reverse electrodialysis, etc.; some emergent technologies for poor regions have been investigated in recent times [6–12 and references therein]. However, cheap and simple point-of-use technologies, for isolated, poor households and small communities, are still necessary to be developed. Generally, methods include an oxidation step to transform As(III) to As(V), which is more easily removed by adsorption and coprecipitation. Thus, many of the works make emphasis on As(III) oxidation; however, most groundwaters of the American region used for drinking purposes are oxic and shallow, with As mainly present in the pentavalent form.

Zerovalent iron technology (ZVI) is a promising method for removal of various pollutants in water and soils, such as chlorinated organics, nitroaromatics, nitrate, azo dyes [13] and metal ions [14,15 and references therein]. Several papers report the efficiency of ZVI to remove As, and different iron materials such as powders, fillings or wires have been tested [16–34]. ZVI reactions are rather slow, but the process can be notably accelerated using iron nanoparticles (NZVI) [35 and references therein]. The tiny particle size, the large surface area and the high density of reactive surface sites (or surface sites of high intrinsic reactivity) lead to a very high efficiency, and make these materials very attractive for remediation; only a few examples of As removal with NZVI have been published, including our own preliminary results. This form of iron was found always much more efficient than other materials [28,32,34,36–38].

The effect of UV or H_2O_2 addition on the ZVI technology, involving Fenton-type processes, has been previously addressed [13,17,39,40]. Studies on UV irradiation, economically promissory because solar light can be used, were generally focused on As(III) oxidation. The SORAS technology (Solar Oxidation and Removal of Arsenic), which uses PET bottles, lemon juice (citrate) and solar light has been tested in natural waters of Bangladesh, Argentina and Chile with different results depending on the water matrix [41–44]. As(III) photooxidation at low pH in the presence of oxygen was analyzed to be applied in remediation of acid mine waters [8]. None of these works considers removal of As in the pentavalent state.

In this paper, As(V) removal by NanoFe®, a new commercial NZVI product, is presented, analyzing the effect of iron mass and the presence of humic acids (HA). For the first time, the effect of UV light irradiation is evaluated in these systems, complemented with the combination of HA plus UV light.

2. Experimental

2.1. Chemicals

As(V) stock solution (1000 mg L^{-1}) was prepared from $NaH_2AsO_4{\cdot}7H_2O$ (Baker). Humic acids (Aldrich, sodium salts, technical) were used. All other chemicals were reagent grade and used without further purification. Water was purified with a Millipore Milli-Q equipment (resistivity = 18 MΩ cm).

Real groundwater samples were obtained from wells of Los Pereyra (Tucumán, Argentina). Synthetic samples, 1 mg L^{-1} As(V), were prepared from the stock solution in controlled ionic composition (CIC) water containing 1.3×10^{-4} M $MgSO_4$, 2.3×10^{-4} M $CaCl_2$, 4.0×10^{-5} M NH_4Cl, 9.0×10^{-6} M $FeCl_3$ and NaOH to adjust pH to 7.8. This composition was similar to that of Los Pereyra waters.

2.2. Synthesis and characterization of NanoFe®

NanoFe® was synthetized by Nanotek S.A. (Santa Fe, Argentina) according to a proprietary novel technology based on chemical reduction of ferric salts with borohydride in a stabilized multiphase nanoemulsion [45].

The product is obtained as an aqueous black suspension, and the particles have magnetic properties. For characterization, the suspension was centrifuged at 2500 rpm for 20 min. The solid was transferred to 3 mL vials under N_2 atmosphere to avoid oxidation, vials were capped with aluminum seal and a silicone *septum*, and kept under N_2 for 24 h. After opening the vials, the samples were dried in a vacuum stove at 40 °C for 24 h. The vials were sealed again and stored in a dry box under N_2 at a very low humidity (<5 ppm).

For XRD analysis, the vial was opened inside the dry box, and a portion of the sample was deposited on the diffraction plate, where it was wetted with absolute ethanol–ethyleneglycol (80:20); the solvent was evaporated at room temperature and the sample was immediately analyzed. A Siemens D5000 diffractometer was used.

For specific surface area measurements, samples were transferred to the equipment (BET surface area analyzer Micromeritics Gemini 2360) under He atmosphere.

The UV–vis spectrum of a NanoFe® sample suspended in 2-propanol was obtained using a Hewlett-Packard diode array UV-visible spectrophotometer, model HP 8453 A.

Samples for transmission electronic microscopy (TEM) were prepared taking a 100–200 μL aliquot of each original aqueous suspension, diluted with deoxygenated water (25 mL) under N_2 bubbling. Some drops of this suspension were deposited on a standard TEM copper grid. The photographs were taken with a TEM Philips EM 301 equipment.

Nanoparticles were stored in 2-propanol until use. Before taking aliquots for any purposes, the 2-propanol suspension was ultrasonicated for 2 min with a Cleanson (25 kHz) ultrasonicator, model CS-1109. The concentration of iron in the suspension, determined by ICP-OES, was 36.6 g L^{-1}.

2.3. Experiments of As removal

In a typical experiment, 150 mL of an As(V) solution (1 mg L^{-1} in CIC water), were introduced into a glass Erlenmeyer 250 mL flask (covered by an aluminum foil in reactions performed in the dark) and bubbled with air (1 mL min^{-1}) for 30 min under orbital stirring at 150 rpm in order to reach oxygen saturation. Then, air bubbling was stopped, and a volume of the NanoFe® 2-propanol suspension containing the corresponding amount of the material (to have final concentrations ranging 0.005–0.1 g L^{-1}) was added, under vigorous and continuous stirring. The flask was left open to the air with continuous stirring until the end of the run. As shaking conditions greatly affect the removal rate of some pollutants by ZVI [46], stirring was carefully controlled in all experiments by setting the orbital stirrer to 150 rpm. In some experiments, humic acids were added at 2 mg L^{-1}.

For light irradiation, a reflector UV lamp (Philips HPA 400S, maximum emission at 365 nm) was positioned 15.5 cm above the top of the flask. The lamp was started immediately after NanoFe® addition. Light intensity, measured with a Spectroline DM-365 XA radiometer at 15.5 cm below the lamp, was 5000 μW cm^{-2}.

Temperature was ambient, without control, and never attained values higher than 30 °C. Initial pH was always 7.8. After the runs, 2.5 mL samples were filtered through a 0.45 μm Millipore membrane and analyzed for As. All experiments were performed at least by duplicate, averaging the results. Errors were never higher than 12%.

Total As in solution was determined by ICP-OES, using a PerkinElmer Optima 3100 XL apparatus. TOC content of samples was measured with a TOC Shimadzu 5000 A instrument in the non-purgeable organic carbon (NPOC) mode.

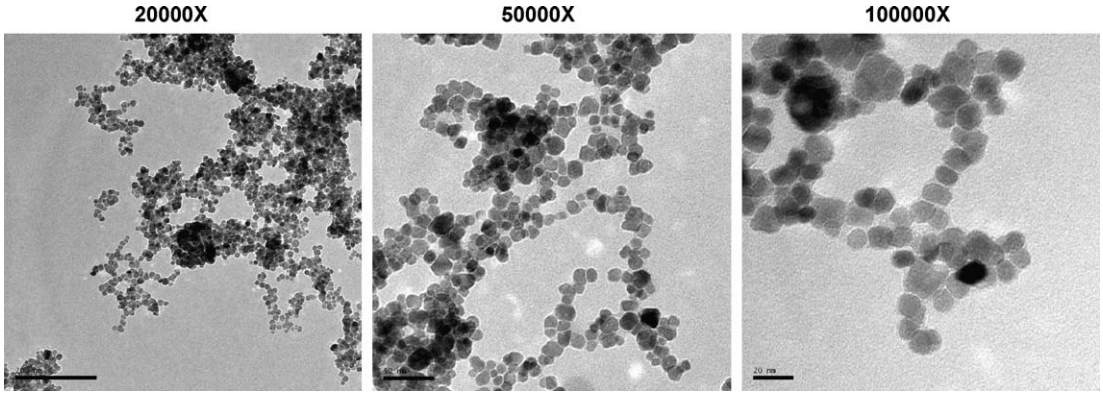

Fig. 1. TEM photographs of NanoFe®.

3. Results and discussion

3.1. Characterization of iron nanoparticles

Three NanoFe® samples (named *S*1, *S*2 and *S*3), obtained in different crops, were tested for characterization. Our results were similar to those reported in the literature [28,34,35].

Diffraction diagrams (not shown) revealed peaks corresponding to zerovalent iron (Fe(0)), maghemite (Fe_2O_3) and magnetite (Fe_3O_4) phases with minor amounts of more amorphous phases.

In Fig. 1, TEM images of the NanoFe® samples are presented as a representative example of different lots. Micrographs show rather regular spherical particles gathered in aggregates in form of chains. At a greater magnification focused on a less aggregated cluster, the closer view allows observation of the morphology of isolated nanoparticles, having a core that could be attributed to zerovalent iron surrounded by a layer of iron oxides. From the comparison between images, combined with the use of the Image-J® software, a particle diameter between 5 and 15 nm for the three analyzed samples, slightly higher for *S*3, was calculated.

Specific surface area was calculated according to the Brunauer–Emmet–Teller (BET) method, using the first three points. Values for the three *S*1, *S*2 and *S*3 samples were 59, 55 and 63 $m^2\,g^{-1}$, respectively. These values are higher than those reported in the literature for other NZVI [28,32,47]. From the obtained S_{BET} area and the density of the material, assuming that particles are spherical and in the same size range, particle size was calculated. Considering that the particles are composed of elemental iron, the calculated radii for *S*1, *S*2 and *S*3 is approximately 7 nm, while if it is assumed that the particles contain iron oxides, the resulting value is approximately 10 nm. These results agree very well with those derived from the scale of the TEM images at different magnifications.

In Fig. 2, the reactive surface can be observed as a function of the particle size. This curve was constructed by calculus, assuming a spherical morphology for the individual particles, which, as shown by TEM images (Fig. 1), is quite a reasonable supposition. Slight differences from this theoretical curve may be found in practice if formation of clusters is considered. These clusters would result in a lower overall specific surface reactivity due to the fact that contact points of neighboring particles are minuscule portions of Fe(0) naked surface that are not available for reaction. As shown by Fig. 2, one special characteristic of nanoparticles is the ability in offering a very high reactivity combined with a low weight.

In Fig. 3, a UV–vis spectrum of a NanoFe® sample in 2-propanol (0.013 M) is shown. The results are quite similar to that obtained for 5 nm iron particles produced within a gel-derived silica glass, showing a high absorption in the short UV region (maximum at 238 nm), which can be attributed to the plasmon resonance of iron nanoparticles, and a small broad absorption between 280 and

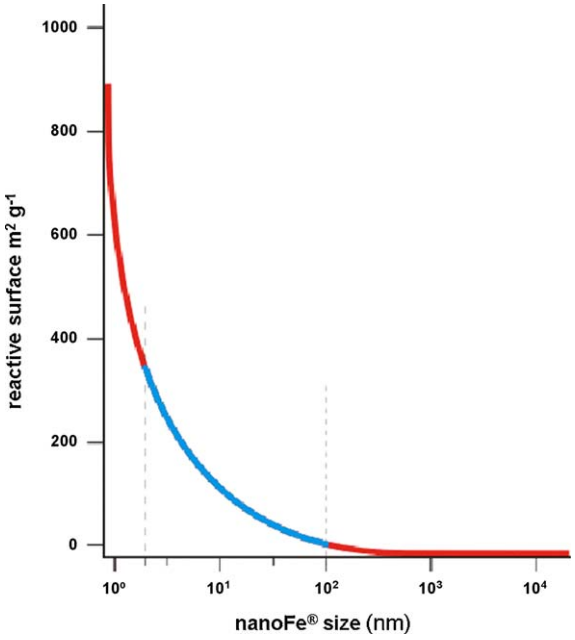

Fig. 2. Plot of the reactive surface as a function of the particle size of NanoFe®.

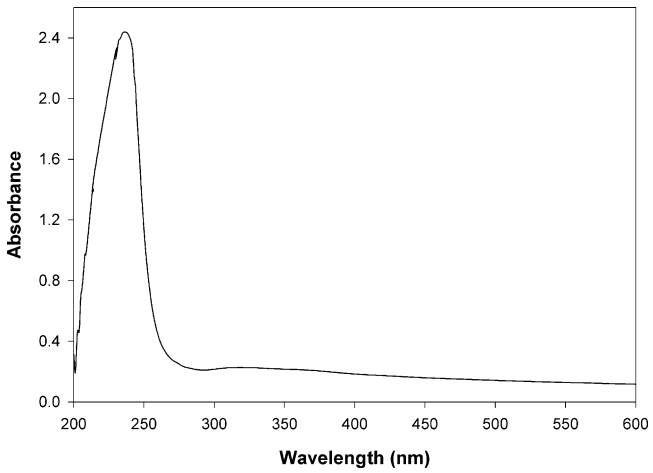

Fig. 3. UV–vis spectrum of NanoFe® in 2-propanol suspension (0.013 M).

600 nm attributed to nanoiron oxide phases [48]. From the spectrum, it can be concluded that the elemental iron moiety does not absorb light emitted by the lamp used in As removal experiments; there will be, however, a very low absorption by the oxide phases of the material. More experiments are underway to shed light on the optical properties of these interesting nanozerovalent iron materials.

3.2. Experiments of As(V) removal with NanoFe® in the dark

Experiments of As(V) removal with NanoFe® were performed always at an initial concentration of 1 mg L^{-1}, which is an upper average value of the As content in well waters of the Chacopampean Plain [37,49]; pH_o was 7.8 in all experiments. In Fig. 4, results of As removal using different NanoFe® concentration are shown. Changes in pH_0 were not significant.

As it can be seen, As removal was rapid and increased with NanoFe® dosage in the range 0.005–0.1 g L^{-1}. Removal attained more than 90% after 150 min of time contact at the highest (NanoFe®) concentrations; 0.05–0.1 g L^{-1} were enough to reach an excellent and rapid efficiency. Similar results, showing an optimal amount of NZVI behind which no improvement of removal was obtained, was shown by Kanel et al. [32], but in our case the optimum mass was lower (see below). In contrast, rather higher doses (0.6–2.5 g L^{-1}) of ordinary iron fillings were necessary to obtain complete As removal in similar conditions [20]. Although in our best conditions final values of As did not still accomplished the required regulation value (10 μg L^{-1}), they surely may be attained with longer contact times with the iron material.

All curves in Fig. 4 could be very well fitted ($R^2 > 0.99$) by biexponential decay functions with a rapid initial decay (~60% in 5 min with the 0.05–0.1 g L^{-1} optimal mass), followed by a slower one. In the table are shown the corresponding fitting parameters: observed rate constants k_1 and k_2 for both exponential decays and surface kinetic rate constants k_{1sa} and k_{2sa}, calculated with an average specific surface area of 60 m^2 g^{-1}. In the inset of Fig. 4, plots of k_1 and k_2 vs. NanoFe® mass are shown and indicate that the first decay time decreases linearly with the increase of Fe concentration; the second decay also varies with mass, but it is less dependent and reaches a saturation. Although k_1 is higher for 0.1 g L^{-1} than for 0.05 g L^{-1}, k_2 are similar, indicating that is the second step that puts a limit in the amount of iron to be used, suggesting that different processes govern the decays. It is important to note that a Langmuir–Hinshelwood kinetic behavior was also tested but it could not be fitted to none of the experimental data.

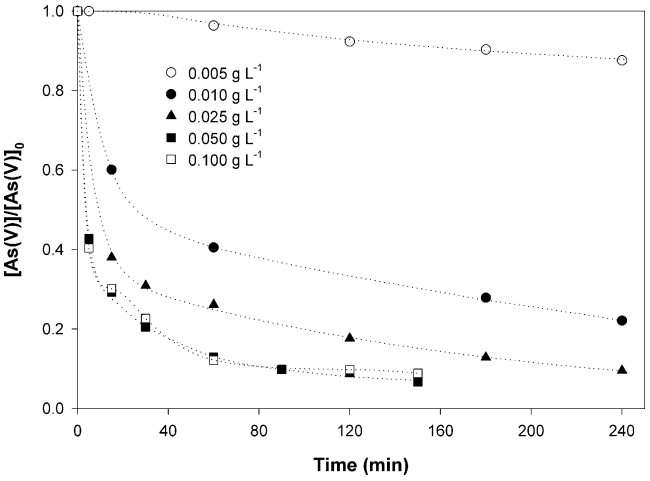

Fig. 4. Time evolution of normalized As concentration during NanoFe® treatment with different iron masses. $[As(V)]_0$ = 1 mg L^{-1} in CIC water; pH_0 7.8. Inset: variation of kinetic rate constants k_1 and k_2 with iron mass (data from Table 1).

NanoFe® proved to be an outstanding material; compared to that of Ref. [32], less mass was necessary to reach an optimal removal, with rate constants one order of magnitude higher. Although our material has a somewhat higher surface area than that of Ref. [32] (60 m^2 g^{-1} vs. 25 m^2 g^{-1}) and lower particle size (7 nm vs. 20 nm), the fact that surface normalized k_{1sa} are one order higher indicates that NanoFe® has an inherent superior activity whose origin is worthwhile to investigate in further works [32]).

Arsenic is a peculiar system compared with others treated by ZVI like nitrate [46], metal ions [50] or bromate [51], where the species are actually reduced by Fe(0). In the case of As(III), oxidation to As(V) is thermodynamically possible [22]; in contrast, although As(V) could be reduced to As(III) at low pH and Eh, there are electrochemical evidences that no reduction takes place under aerobic conditions, unless the iron material in contact with arsenical solutions for several days [19,22,32]. Removal of As(V) occurs without changes in the oxidation state, predominantly by adsorption on iron oxide species generated *in situ* by corrosion of zerovalent iron and further coprecipitation. In the presence of oxygen as electron acceptor, Fe(0) decomposes water with formation of ferrous ions:

$$2Fe(0) + 2H_2O + O_2 \rightarrow 2Fe(II) + 4HO^- \quad (1)$$

Although corrosion is favored at low pH, reaction (1) still takes place relatively rapidly at pH 7–8. Once formed, Fe(II) reacts with dissolved O_2 generating Reactive Oxygen Species (ROS) like $HO^\bullet$, $O_2^{\bullet-}/HO_2^\bullet$, H_2O_2, and is oxidized to Fe(III). Simplified equations follow for neutral pH [31]:

$$Fe(II) + O_2 \rightarrow Fe(III) + O_2^{\bullet-} \quad (2)$$

$$Fe(II) + O_2^{\bullet-} + 2H^+ \rightarrow Fe(III) + H_2O_2 \quad (3)$$

$$2O_2^{\bullet-} + 2H^+ \rightarrow H_2O_2 + O_2 \quad (4)$$

$$H_2O_2 + O_2^{\bullet-} \rightarrow HO^\bullet + O_2 + HO^- \quad (5)$$

$$Fe(II) + O_2^{\bullet-} + 2H^+ \rightarrow Fe(III) + H_2O_2 \quad (6)$$

$$Fe(II) + H_2O_2 \rightarrow Fe(III) + HO^\bullet + HO^- (\text{Fenton reaction}) \quad (7)$$

Species of higher oxidation state like Fe(IV) were also proposed, especially at neutral pH. Global reactions are:

$$Fe(II) + 1/4O_2 + 1/2H_2O \rightarrow Fe(III) + HO^- \quad (8)$$

$$Fe(III) + 3H_2O \rightarrow Fe(OH)_3 + 3H^+ \quad (9)$$

Eq. (9) indicates that Fe(III) precipitation is enhanced in less acid media. Different Fe(II)/(III) oxides or hydr(oxides) such as iron rusts, magnetite, lepidocrocite, maghemite, etc. are formed as corrosion products, which will be called here generically ferric (or ferrous) oxides, "FeO_x", irrespective of their crystallinity or chemical form. Fe(II) adsorption on the formed "FeOx" accelerates autocatalytically the process [31]. The iron corrosion products constitute an excellent adsorbent for As(V), a process promoted in aerobic environments [16–19,22,31,32,52]. Adsorption on "FeOx" takes place through a variety of mechanisms like electrostatic attraction, ion exchange, complexation, physisorption, etc., described by several models [26,53]. It has been proposed that As(V/III)–Fe inner-sphere complexes of different structure are formed, which can even migrate inside the iron structure [19,52,54]; for adsorption of As(V) on goethite, it has been

suggested that two successive steps take place involving the formation of monodentate and bidentate inner-sphere complexes [19]. As a final result, As species will be removed from the solution by adsorption/coprecipitation on fresh "FeOx" formed *in situ*. Thus, once formed, minor amounts of Fe(II) trigger a continuous cycle of oxidation and reduction of Fe(II)/Fe(III) species that improves the whole process.

The double exponential decay observed in Fig. 4 could be explained by different factors such as changes with time of ligand exchange reactions [28] (e.g., formation of different As(V) complexes on the "FeOx" surface), appearance of different active sites for adsorption or changes in some other surface properties.

3.3. Experiments of as removal with NanoFe® in the presence of humic acids

Humic acids (HA) are representative of natural organic matter (NOM) and are the primary light-absorbing species in natural aquatic environment [55]. HA interferes with adsorption of As species on "FeOx" and hence influences their mobility in water [54]. Thus, it is essential the evaluation of the presence of these substances in natural groundwater when NZVI is intended to be used for As removal.

In Fig. 5, results of As removal with NanoFe® at two different concentrations, showing the influence of HA addition (2 mg L^{-1}), are presented. This concentration corresponds to 0.62 mg L^{-1} of carbon, as measured by TOC. As it can be seen, HA are detrimental, decreasing around 50% the removal efficiency. Decay of As concentration follows again a biexponential decay. The respective rate constants are shown in Table 1, and the values perfectly reflect the inhibition: both k_{1sa} and k_{2sa} are half the values in the presence of HA. A similar trend was observed by Giasuddin et al. [34].

Humic acids contain significant proportions of aliphatic and aromatic carboxylate, phenolic, carbonyl groups and other functions [54,56]. The inhibiting effect of HA in ZVI systems [34,50,57] has been attributed to occupancy or obstruction of active sites by HA by adsorption, complexation of HA with Fe(0) (and "FeOx") and reduction of iron corrosion rates, decreasing the probability of formation of new adsorption sites. Even enhanced coagulation of NZVI by HA has been mentioned to take place [34]. Taking into account that pzc's of "FeOx" are generally higher than 6 [32,53], adsorption of HA at pH 7.8 on the iron phases will take place predominantly through the phenolic groups, which are still protonated [56]. Moreover, when metal ions like Fe are present in natural HA, metal-bridge combination between HA and As species diminishes the trend of dissolved anions (like arsenate) to form surface complexes; even desorption of arsenical species from "FeOx" used as sorbents can take place [54]. All these factors make HA adsorption generally dominant over that of other chemical species.

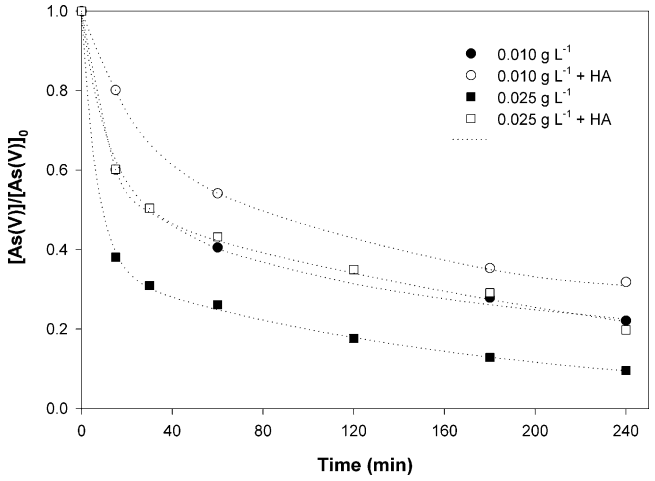

Fig. 5. Time evolution of normalized As concentration during NanoFe® treatment with different iron masses without and with HA addition. $[As(V)]_0$ = 1 mg L^{-1}; [HA] = 2 mg L^{-1}; pH_0 7.8.

3.4. Experiments of As removal with NanoFe® under UV irradiation in the absence and in the presence of HA

Effect of UV light on As removal with ZVI (including the effect of HA addition) has been not previously studied with the exception of our own exploratory experiments [36–38]. In Fig. 6, results of As removal using NanoFe® with two different masses under UV light irradiation without and with HA addition are presented. For comparison, data in the dark are also presented. In all cases, it is clear that UV irradiation enhances As removal. In the absence of HA and as in the previous cases, the kinetic behavior followed a biexponential decay and Table 1 indicates the values of rate parameters. Rate constants for the first exponential decays (k_1) under UV are practically twofold those in the dark, indicating that the beneficial effect of the light can be ascribed to species generated by illumination. On the contrary, k_2 is less dependent.

Neither As(V) nor Fe(0) (Fig. 3) absorb in the working wavelength, thus the photochemical process must be ascribed to another chromophore. Iron oxides initially present in NanoFe® and Fe(II)/Fe(III) produced after Fe corrosion (either in solution or at the interface) might be then responsible for light effects [42,58,59 and references therein]. One possibility may be $HO^{\bullet}$ photoproduction from Fe(III)–hydroxycomplexes:

$$Fe(III)OH^{2+} + h\nu \rightarrow HO^{\bullet} + Fe(II) \quad (10)$$

but quantum yield of this reaction is very low [42]. Other processes might be originated in the role of "FeOx" as semiconductors (bandgaps around 2 eV) [60], according to the following simplified equations, which indicate additional ROS formation and participation of Fenton reactions like (7) [58]:

$$\text{"FeOx"} + h\nu \rightarrow e_{cb}^{-} + h_{vb}^{+} \quad (11)$$

$$HO^{-}(H_2O) + h_{vb}^{+} \rightarrow HO^{\bullet}(+H^{+}) \quad (12)$$

$$O_2 + e_{cb}^{-}(+H^{+}) \rightarrow O_2^{\bullet -}(HO_2^{\bullet}) \quad (13)$$

$$O_2 + e_{cb}^{-} + H_2O_2 \rightarrow HO^{\bullet} + HO^{-} \quad (14)$$

$$Fe(III) + e_{cb}^{-} \rightarrow Fe(II)$$

As reported in the previous section, HA caused a detrimental effect on As(V) removal in the dark. Under UV irradiation it can be observed that HA actually inhibited removal during the first stages

Table 1
Kinetic and surface area normalized rate constants for biexponential decay of normalized As concentrations extracted from data of Fig. 4.

[NanoFe®] (g L^{-1})	k_1 (min^{-1})	k_2 (min^{-1})	k_{1sa} (min^{-1} m^{-2} L)	k_{2sa} (min^{-1} m^{-2} L)
0.005	0.0031	0.0028	0.0103	0.0094
0.010	0.0879	0.0025	0.1465	0.0042
0.010 + HA	0.0445	0.0095	0.0074	0.0016
0.010 + UV	0.1556	0.0013	0.2594	0.0022
0.025	0.1452	0.0059	0.0968	0.0040
0.025 + HA	0.0796	0.0029	0.0531	0.0019
0.025 + UV	0.3512	0.0111	0.2342	0.0074
0.050	0.4511	0.0305	0.1594	0.0102
0.100	0.8460	0.0349	0.1410	0.0058

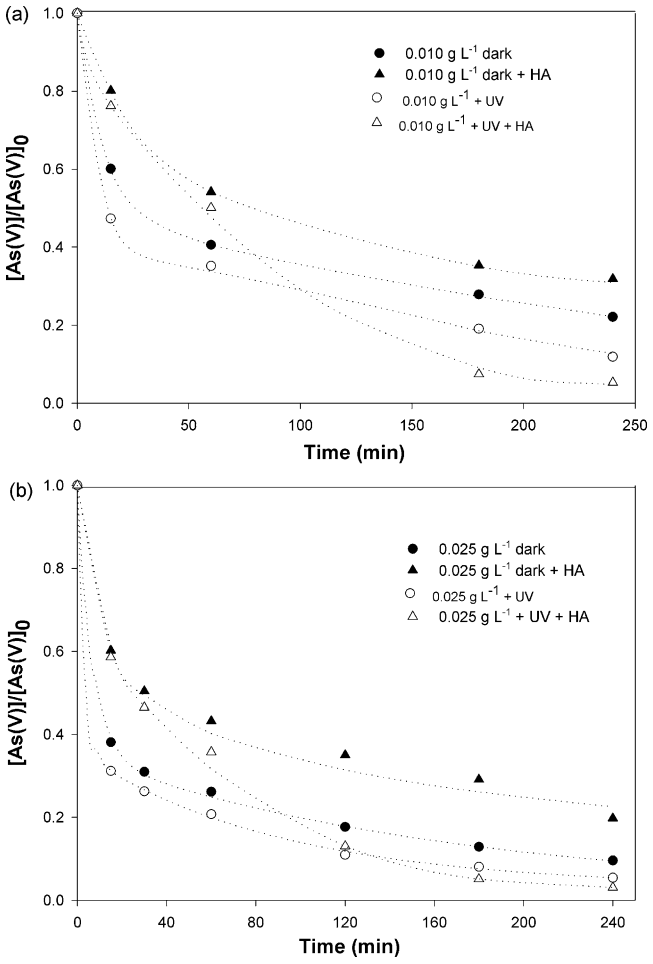

Fig. 6. Time evolution of normalized As concentration during the NanoFe® treatment with different iron masses under UV irradiation, without and with HA addition. $[As(V)]_0 = 1\ mg\ L^{-1}$; $[HA] = 2\ mg\ L^{-1}$; pH_0 7.8; light intensity (365 nm) = 5000 μW cm^{-2}. (a) Experiments with $0.010\ g\ L^{-1}$; (b) experiments with $0.025\ g\ L^{-1}$. Experiments in the dark are shown for comparison.

of irradiation but, after a period, the rate increased yielding a final removal rather higher than that in the absence of HA: an almost complete As removal at 240 min was reached for both cases, with 0.010 and $0.025\ g\ L^{-1}$ of NanoFe®, a behavior not observed in any of the other cases. Moreover, a different kinetic behavior (probably more complicated) is observed in the curves, which for this reason were not modeled. For this reason, kinetic rate constants for these conditions are not included in Table 1. No efforts were made in the present work to study the optimal amount of HA that improves As removal.

In order to explain the role of HA, different pathways may participate in the process of As removal, being difficult to be discriminated. This complex kinetics is reflected in the difficulty of modeling curves of Fig. 6. HA are able to produce ROS in the presence of UV light and oxygen [55,58,61,62 and references therein], although ROS formation may proceed with low quantum yields [63]. Alternatively, HA or its excited state (HA*) behaving as organic carboxylates, form complexes with dissolved and surface Fe(III) species, which through light absorption participate in LMCT reactions where the organic moiety is oxidized and Fe(III) is reduced with further dissolution; this includes participation of photo-Fenton type reactions (Eq. (7)):

$$HA + h\nu \rightarrow HA^{*}(\text{singlet or triplet}) \quad (15)$$

$$HA^{*} + O_2 \rightarrow \text{Products} + O_2^{\bullet -}/HO_2^{\bullet} \quad (16)$$

$$O_2^{\bullet -}/HO_2^{\bullet} \rightarrow H_2O_2 \quad (17)$$

$$[Fe(III) - HA(HA^{*})]_{diss}/ > [Fe(III){-}HA(HA^{*})]_{surf} + h\nu \rightarrow Fe(II) + HA^{\bullet +} \rightarrow \text{HA oxidation products} \quad (18)$$

Finally, the action of "FeOx" as semiconductors, generate electrons through reaction (11), promoting also iron dissolution by electron attack to Fe(III) [64]:

$$e_{cb}^{-} + > Fe(III) \rightarrow > Fe(II) \rightarrow Fe(II)_{diss} \rightarrow Fe(III)_{diss} \quad (19)$$

This reaction will produce the consequent photocatalytic oxidation of HA by $HO^{\bullet}$ or h_{vb}^{+}, as reported to occur with TiO_2 or mixed TiO_2–Fe_2O_3 photocatalysts [65,66].

Then, reactions (2)–(7) take place. Reaction (18) promotes formation of other radical species, some of them strong reductants that may drive additional Fe(III) and O_2 reductions. Here, the possibility of As(V) reduction to As(III) (and further reoxidation) by reductive radicals cannot be ruled out. Peroxyl radicals or tetraoxides, formed from organic radicals and O_2, can take part also in this complex system.

Similarly to the cases in the dark, NanoFe® mass influences reaction rate in all conditions, indicating the relevance of the number of reactive sites on the metal surface as the principal responsible for the reaction. All the mentioned processes will contribute to the formation of nascent iron oxides on the surface of nanozerovalent iron, improving sensibly As(V) adsorption and removal.

In the studies on As removal under UV (or solar irradiation) in the presence of citrate, it was noticed that citrate photoproducts promoted flocculation and precipitation of Fe(III), improving As removal [42,43]. On the other hand, an induced flocculation of nanoparticles stabilized by photolabile agents was observed under UV light, provoking a change in interfacial chemical composition and hence decreasing the efficiency of surface stabilizing layers [67,68]. This photoflocculation could be caused here by the phototransformation of HA or Fe(III)–HA complexes.

3.5. Experiments with real well waters

Results described in previous sections encouraged us to test real well waters of Los Pereyra (East of the Tucumán Province, Chacopampean Plain, Salí River hydrogeological basin [37]). The quality of shallow groundwater, used for drinking purposes, is poor due to high bacteriological content, high salinity and high levels of nitrates, boron, fluoride and traces of manganese and arsenic [49]. Waters are predominantly oxic, with high pH values (7.0–8.7); for this reason, arsenic – coming from metal oxides in the sediments or from dissolution of volcanic glass – should be mainly present as As(V). Concentrations were well above the $10\ \mu g\ L^{-1}$ regulation ($200–1000\ \mu g\ L^{-1}$). There is a high incidence of water-borne diseases in the region, including HACRE.

In previous works [37,43], the efficiency of SORAS was tested in these waters, finding a poor removal efficiency (around 30%) compared with that obtained with synthetic waters of similar composition. The main factor of failure was the low original iron concentration in the waters, being necessary to add iron externally before the treatment; some typical iron-containing materials of the zone were tested, with dissimilar results. Also, the chemical matrix of water and changes in the operative conditions altered unpredictably SORAS efficiency. It was proved that addition of lemon juice was not strictly needed, but the effect of sunlight was generally beneficial. Preliminary experiments indicated that NanoFe® was a better iron source than other tested iron materials [36–38].

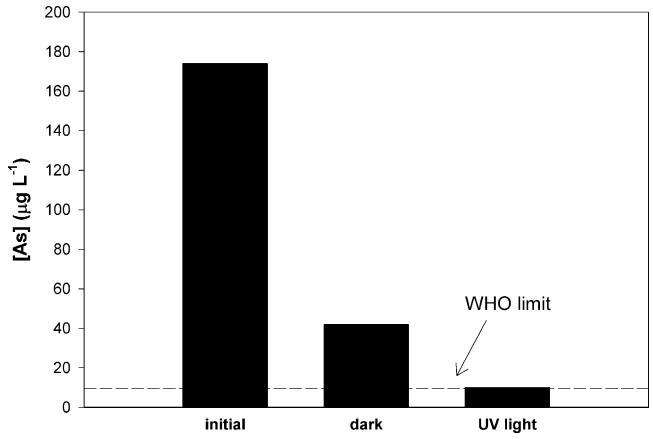

Fig. 7. As removal by NanoFe® in real waters of Los Pereyra. Irradiation time: 3 h; [NanoFe®] = 0.025 g L^{-1}; pH_0 7.9; light intensity (365 nm) = 5000 μW cm^{-2}.

Results of treatment of water from Los Pereyra with NanoFe® are shown in Fig. 7. From an initial As concentration of 174 μg L^{-1}, a rather good removal was obtained in the dark (76%), but results were very much improved after 3 h under UV irradiation, attaining levels of As well in agreement with regulations (<10 μg L^{-1}). No efforts to establish the exact oxidation state of As (tri- or pentavalent) in the sample were made. However, the efficiency of the method does not seem to depend on As speciation. This contrasts with results obtained in waters from Bangladesh and India, probably because no light was used in the treatment and because Asian SE waters contain predominantly As(III) [32]. The amount of NanoFe® used in the experiment (0.025 g L^{-1}) was even lower than the optimum found in the runs with synthetic waters. In addition, the TOC content of the sample was 130 mg L^{-1}, very much higher than that used in experiments with laboratory prepared samples (0.62 mg L^{-1}). This indicates the important improvement of the As removal efficiency by NOM.

4. Conclusions

Use of NanoFe® resulted in outstanding results on synthetic CIC waters spiked with As. Characterization of the commercial material indicated that it was composed of rather regular spherical particles (5–15 nm), with specific surface area around 60 m^2 g^{-1}, i.e., higher than other reported NZVI in the literature. Phases of elemental Fe and iron oxides were observed by XRD. TEM photographs indicated regular particles gathered in chain aggregates. This material seemed promissory for As removal, due to the higher contact area which could be established between phases.

Experiments with arsenical solutions revealed that a rather low NanoFe® mass (0.05–0.1 g L^{-1}) was enough to attain an excellent removal (more than 90% after 150 min), making the method convenient from an economical point of view. HA was detrimental, decreasing removal around 50%. In contrast, UV light doubled removal rates; the process was even more enhanced in the presence of HA, with an almost total arsenic removal within 4 h.

Although the superior activity may be attributed to the high surface area of the nanoparticles, an intrinsic superior reactivity of the iron sample was additionally observed, higher than that of other reported NZVI. Due to the low amount of iron used, the mass of wastes produced in the process is significantly low; additionally, the flocs might be removed by magnetic techniques, often more efficient and faster than centrifugation or filtration. This adds two important technological advantages.

The present work focused on removal of As in the pentavalent state, characteristic of most Latin-American groundwaters. The effect of light irradiation has been analyzed. It was proved that humic acids, which inhibited removal in the dark, very much improved the reaction in the presence of light, due to the formation of very reactive species that enhance corrosion processes. This was confirmed by the high efficiency of As removal in real well waters of Los Pereyra, having high NOM content.

In further studies, more refined kinetic experiments will be performed, comprising identification of reactive intermediates, and including removal of As(III), together with the effect of interfering cations or anions.

Preliminary results with NanoFe® on natural well waters are very promissory. Under UV irradiation for 3 h, As contents in agreement with the regulations (<10 μg L^{-1}) were obtained, using a NanoFe® mass lower than in the experiments with synthetic waters. More studies with other samples of different source or extracted from wells of different depths are mandatory to validate the technology, as the physicochemical properties of the samples can extremely affect the removal efficiency.

Acknowledgements

This work was performed as part of Agencia Nacional de Promoción Científica y Tecnológica (ANPCYT) PICT03-13-13261 and PICT 00512 Projects. To IBEROARSEN CYTED 406RT0282 Network for additional support. To Prof. María Isabel Pividori, Grup de Sensors & Biosensors, Unitat de Química Analítica, Universitat Autònoma de Barcelona, Bellaterra, Barcelona – Spain for TEM micrographs. To Lic. Gisela Pagano, Nanotek SA, for the synthesis of the iron nanoparticles. MIL is a member of CONICET. MEM and IKL thank CONICET for postdoctoral and doctoral fellowships, respectively. VS thanks ANPCYT for a doctoral fellowship.

References

[1] Prospect of Rural Latin American Communities for Application of Low-cost Technologies for Water Potabilization, OAS Project AE 141/2001, M.I. Litter (Editor), Digital Grafic, La Plata. http://www.cnea.gov.ar/xxi/ambiental/agua-pura/default.htm, 2002.
[2] J. Bundschuh, B. Farias, R. Martin, A. Storniolo, P. Bhattacharya, J. Cortes, G. Bonorino, R. Albouy, Appl. Geochem. 19 (2004) 231.
[3] World Health Organization, Guidelines for drinking water quality, vol. 1, Recommendations, 3rd ed., Geneva, 2004.
[4] Código Alimentario Argentino, modification of articles 982 and 983, Buenos Aires, Argentina. http://www.anmat.gov.ar/normativa/normativa/Alimentos/Resolucion_Conj_68-2007_96-2007. pdf, May 22, 2007.
[5] P.L. Smedley, H.B. Nicolli, D.M.J. Macdonald, A.J. Barros, J.O. Tullio, Appl. Geochem. 17 (2002) 259.
[6] http://www.epa.gov/safewater/arsenic.htm.
[7] J.G. Hering, P.-Y. Chen, J.A. Wilkie, M. Elimelech, J. Environ. Eng. 8 (1997) 800.
[8] M.T. Emmett, G.H. Khoe, Water Res. 35 (2001) 649.
[9] M. Driehaus, M. Jekel, U. Hildebrandt, J. Water SRT-Aqua 47 (1998) 30.
[10] L. Cumbal, A.K. SenGupta, Environ. Sci. Technol. 39 (2005) 6508.
[11] M.E. Pena, G.P. Korfiatis, M. Patel, L. Lippincott, X. Meng, Water Res. 39 (2005) 2327.
[12] B. Robintson, C. Duwig, N. Bolan, M. Kannathasan, A. Saravanan, Sci. Total Environ. 301 (2003) 67.
[13] N. Deng, F. Luo, F. Wu, M. Xiao, X. Wu, Water Res. 34 (2000) 2408.
[14] R.M. Powell, R.W. Puls, S.K. Hightower, D.A. Sabatini, Environ. Sci. Technol. 29 (1995) 1913.
[15] M.I. Litter, in: P. Boule, D.W. Bahnemann, P.K.J. Robertson (Eds.), The handbook of environmental chemistry, vol. 2. Part M, Environmental Photochemistry Part II, Springer-Verlag, Berlin-Heidelberg, 2005, p. 325.
[16] J.A. Lackovic, N.P. Nikolaidis, G.M. Dobbs, Environ. Eng. Sci. 17 (2000) 29.
[17] M.V. Balarama Krishna, K. Chandrasekaran, D. Karunasagar, J. Arunachalam, J. Hazard. Mater. B84 (2001) 229.
[18] J. Farrell, J. Wang, P. O'Day, M. Conklin, Environ. Sci. Technol. 35 (2001) 2026.
[19] C. Su, R.W. Puls, Environ. Sci. Technol. 35 (2001) 1487.
[20] A. Ramaswami, S. Tawachsupa, M. Isleyen, Water Res. 35 (2001) 4474.
[21] C. Su, R.W. Puls, Environ. Sci. Technol. 35 (2001) 4562.
[22] N. Melitas, M. Conklin, J. Farrell, Environ. Sci. Technol. 36 (2002) 3188.
[23] B.A. Manning, M.L. Hunt, C. Amrhein, J.A. Yarmoff, Environ. Sci. Technol. 36 (2002) 5455.
[24] S.J. Morrison, D.R. Metzler, B.P. Dwyer, J. Contam. Hidrol. 56 (2002) 99.
[25] N.P. Nikolaidis, G.M. Dobbs, J.A. Lackovic, Water Res. 37 (2003) 1417.

[26] S. Bang, G.P. Korfiatis, X. Meng, J. Hazard. Mater. 121 (2005) 61.
[27] S. Bang, M.D. Johnson, G.P. Korfiatis, X. Meng, Water Res. 39 (2005) 763.
[28] S.R. Kanel, B. Manning, L. Charlet, H. Choi, Environ. Sci. Technol. 39 (2005) 1291.
[29] Y. Zhang, C. Amrhein, W.T. Frankenberger Jr., Sci. Total Environ. 350 (2005) 1.
[30] H.-L. Lien, R.T. Wilkin, Chemosphere 59 (2005) 377.
[31] O.X. Leupin, S.J. Hug, Water Res. 39 (2005) 1729.
[32] S.R. Kanel, J.M. Greneche, H. Choi, Environ. Sci. Technol. 40 (2006) 2045.
[33] H. Sun, L. Wang, R. Zhang, J. Sui, G. Xu, J. Hazard. Mater. B129 (2006) 297.
[34] A.B.M. Giasuddin, S.R. Kanel, H. Choi, Environ. Sci. Technol. 41 (2007) 2022.
[35] J.T. Nurmi, P.G. Tratnyek, V. Sarathy, D.R. Baer, J.E. Amonette, K. Pecher, C. Wang, J.C. Linehan, D.W. Matson, R.L. Penn, M.D. Driessen, Environ. Sci. Technol. 39 (2005) 1221.
[36] M.E. Morgada, M. Mateu, J. Bundschuh, M.I. Litter, e-Terra, http://e-terra@geopor.pt, vol. 5, no. 5, 2008, ISSN 1645-0388.
[37] J. ́dHiriart, M. del V. Hidalgo, M.G. García, M.I. Litter, M.A. Blesa, in: J. Bundschuh, M.A. Armienta, P. Bhattacharya. J. Matschullat, P. Birkle, Arun B. Mukherjee (eds.), Natural Arsenic in Groundwater of Latin America—Occurrence, Health Impact and Remediation, vol. 1. Balkema Publisher, Lisse, The Netherlands, Interdisciplinary Book Series: ''Arsenic in the Environment'', Series Editors: J. Bundschuh, P. Bhattacharya, A.A. Balkema Publishers, Taylor and Francis Publishers, 2008, pp. 615–624.
[38] M.E. Morgada de Boggio, I.K. Levy, M. Mateu, P. Bhattacharya, J. Bundschuh, M.I. Litter, in: J. Bundschuh, M.A. Armienta, P. Bhattacharya, J. Matschullat, P. Birkle, A.B. Mukherjee (eds.), Natural Arsenic in Groundwater of Latin America—Occurrence, Health Impact and Remediation, vol. 1, Balkema Publisher, Lisse, The Netherlands, Interdisciplinary Book Series: ''Arsenic in the Environment'', Series Editors: J. Bundschuh, P. Bhattacharya, A.A. Balkema Publishers, Taylor and Francis Publishers, 2008, pp. 677–686.
[39] C.O. Pulgarin, J.-P. Schwitzguebel, P.A. Peringer, J. Adv. Oxid. Technol. 1 (1996) 94.
[40] M.-C. Chang, H.-Y. Shu, H.-H. Yu, J. Hazard. Mater. 138 (2006) 574.
[41] S. Hug, EAWAG News, 49, 18–20, December 2000.
[42] S.J. Hug, L. Canonica, M. Wegelin, D. Gechter, U. Von Gunten, Environ. Sci. Technol. 35 (2001) 2114.
[43] M.G. García, J. d'Hiriart, J. Giulitti, H. Lin, G. Custo, M.V. Hidalgo, M.I. Litter, M.A. Blesa, Solar Energy 77 (2004) 601.
[44] F. Lara, L. Cornejo, J. Yañez, J. Freer, H.D. Mansilla, J. Chem. Technol. Biotechnol. 81 (2006) 1282.
[45] http://www.nanoteksa.com.
[46] C.-H. Liao, S.-F. Kang, Y.-W. Hsu, Water Res. 37 (2003) 4109.
[47] C.B. Wang, W. Zhang, Environ. Sci. Technol. 31 (1997) 2154.
[48] S. Basu, D. Chakravorty, J. Non-Crystal. Solids 352 (2006) 380.
[49] C. Navntoft, P. Araujo, M.I. Litter, M.C. Apella, D. Fernández, M.E. Puchulu, M. del, V. Hidalgo, M.A. Blesa, J. Solar Energy Eng. 129 (2007) 127.
[50] S.M. Ponder, J.G. Darab, T.E. Mallouk, Environ. Sci. Technol. 34 (2000) 2564.
[51] L. Xie, C. Shang, Environ. Sci. Technol. 39 (2005) 1092.
[52] J.T. Mayo, C. Yavuz, S. Yean, L. Cong, H. Shipley, W. Yu, J. Falkner, A. Kan, M. Tomson, V.L. Colvin, Sci. Technol. Adv. Mater. 8 (2007) 71.
[53] S. Dixit, J.G. Hering, Environ. Sci. Technol. 37 (2003) 4182.
[54] A.D. Redman, D.L. Macalady, D. Ahmann, Environ. Sci. Technol. 36 (2002) 2889.
[55] X. Ou, S. Chen, X. Quan, H. Zhao, Chemosphere 72 (2008) 925.
[56] D.G. Lumsdon, A.R. Fraser, Environ. Sci. Technol. 39 (2005) 6624.
[57] E.J. Weber, Environ. Sci. Technol. 30 (1996) 716.
[58] M.I. Litter, Appl. Catal. B: Environ. 23 (1999) 89.
[59] B.M. Voelker, F.M.M. Morel, B. Sulzberger, Environ. Sci. Technol. 31 (1997) 1004.
[60] M.I. Litter, J.A. Navío, J. Photochem. Photobiol. A 84 (1994) 183.
[61] P.L. Miller, Y.-P. Chin, J. Agric. Food Chem. 50 (2002) 6758.
[62] D. Vione, G. Falletti, V. Maurino, C. Minero, E. Pelizzetti, M. Malandrino, R. Ajassa, R.I. Olariu, C. Arsene, Environ. Sci. Technol. 40 (2006) 3775.
[63] P.P. Vaughan, N.V. Blough, Environ. Sci. Technol. 32 (1998) 2947.
[64] M.I. Litter, J.A. Navío, J. Photochem. Photobiol. A 98 (1996) 171.
[65] J. Wiszniowski, D. Robert, J. Surmacz-Gorska, K. Miksch, J.-V. Weber, J. Photochem. Photobiol. A 152 (2002) 267.
[66] S. Qiao, D.D. Sun, J.H. Tay, C. Easton, Water Sci. Technol. 47 (2003) 211.
[67] A. Vesparinas, J. Eastoe, S. Jackson, P. Wyatt, Chem. Commun. (2007) 3912.
[68] A. Salabat, J. Eastoe, A. Vesparinas, R.F. Tabor, K.J. Mutch, Langmuir 24 (2008) 1829.